# STRUCTURAL PERFORMANCE EVALUATION OF THE Dura-Bridge® AND MONITORING SYSTEM APPLICATION

## 超高耐久橋梁 Dura-Bridge®の性能評価と常時モニタリングの概要

構造技術部　ホアン チョン クエン　HOANG TRONG KHUYEN
構造技術部　野並 優二　YUUJI NONAMI
構造技術部　藤岡 泰輔　TAISUKE FUJIOKA
構造技術部　内堀 裕之　HIROYUKI UCHIBORI

コンクリート道路橋では，経年劣化や塩害等による腐食劣化に起因した耐久性の著しい低下や維持管理の負担増加が課題となっており，抜本的な解決策が求められている。そこで，腐食劣化の根源となる鉄筋やPC鋼材を一切使用せず，非腐食材料のみで構造を成立させた超高耐久橋梁を開発し，高速道路橋の別埜谷橋に適用した。この超高耐久橋梁の長期健全性を把握することを目的として，建設直後において総重量40t級の車両静的載荷試験により，ひずみや変位から設計・施工の妥当性を確認した。また，車両落下の動的載荷試験による加振から橋梁の振動特性と外ケーブル張力計測の基礎データを収集した。長期的な性能を評価するため，本橋に設置・運用した自動モニタリングシステムについて述べる。
キーワード：　超高耐久橋梁，非鉄製，静的載荷実験，動的載荷実験，モニタリング

A significant decrease in the durability of concrete bridges due to aging and salt damage is a severe problem recently. To solve this problem, the Dura-Bridge®, that using only non-corrosive materials without using any reinforcing bars or PC steel materials that are the source of corrosion deterioration, has been developed. This type of bridge has been first applied as highway bridges in the Bessodani Bridge. To understand the long-term performance and to validate the design, the bridge was statically tested by verifying strain and displacement under the static loading of a total weight of 40-ton vehicle loaded immediately after construction. In addition, the bridge vibration characteristics and external cable tension measured from vibration were recorded to form foundation data for long-term monitoring by a dynamic test of dropping the vehicle. The automated real-time monitoring system which was installed and put in operation at the bridge was explained in this paper.
***Key Words***: Ultra-durable bridge, Nonmetallic, Static testing, Dynamic testing, Monitoring

## 1.　INTRODUCTION

The first prestressed concrete bridges date back to almost a hundred years ago, and innovation in PC bridge technology is still accelerating. PC bridges are supposed to require less maintenance work than steel bridges, but their steel strands, rebar are susceptible to be corroded. Beginning with the non-metallic concept of using only non-corrosive materials, avoiding the use of rebars or PC steel strands that cause corrosion deterioration, the ultra-high durability bridge, the Dura-Bridge®, was developed[1]. This non-metallic PC bridge is invented as a result of the development of fiber-reinforced concrete and butterfly web structures[2], together with applying the outcomes of research into aramid fiber reinforced polymer, AFRP tendons[3] conducted since the 1990s. With ultra-high durability, this type of bridge is expected as a solution for not only solving the demand of reducing maintenance issues in Japan but also forming sustainable infrastructures.

The world’s first expressway bridge constructed as an

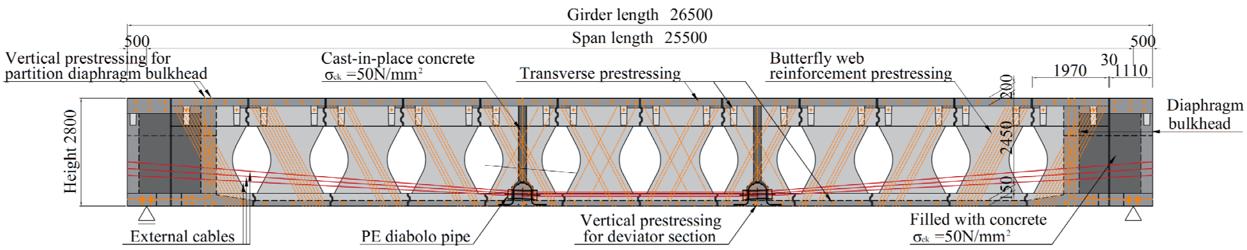


(a) Side view

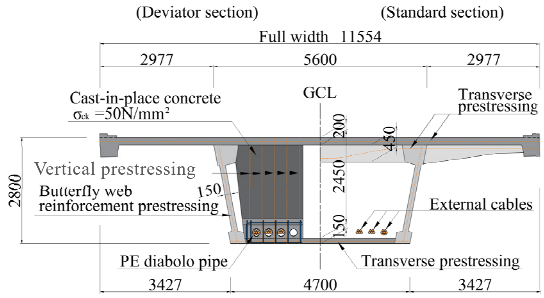


(b) Cross section

Primary materials:

- Precast concrete $\sigma_{ck}$=80 N/mm$^2$
- Cast in plate concrete $\sigma_{ck}$=50 N/mm$^2$
- AFRP rod nominal diameter 7.4mm
- Rod guaranteed strength 81.4kN/rod

(c) Aramid fiber reinforced polymer, AFRP

**Fig. 1.** The Bessodani Bridge

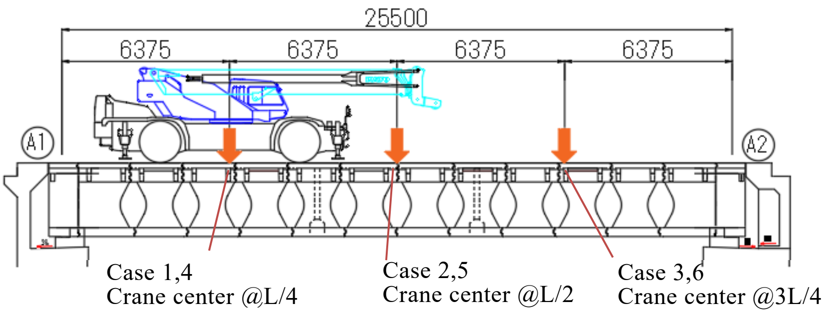


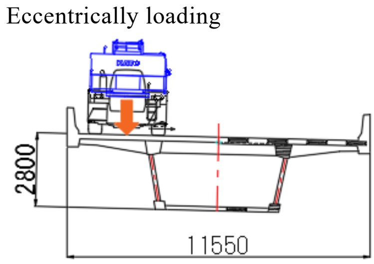


(a) Test longitudinal direction

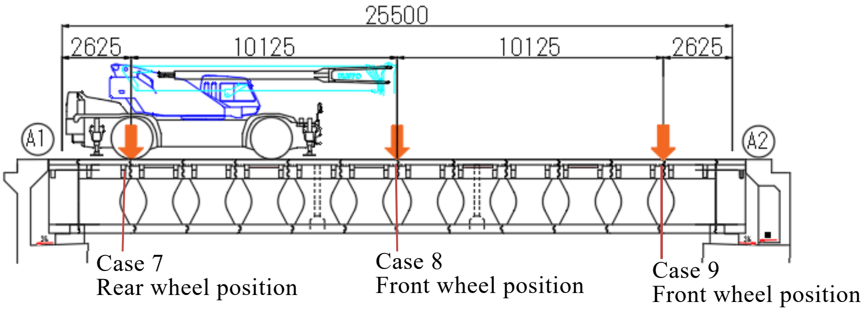


(b) Test segmental joints

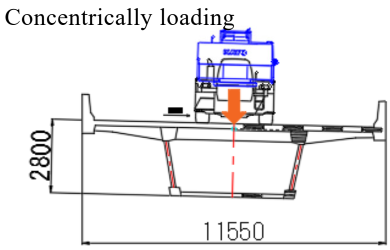


(c) Load position on deck slab

Loading information:
Crane: KATO SL-650R; Gross Weight: 39595kg;
Front wheel: 19710kg; Rear wheel: 19885kg

**Fig. 2.** Loadings for static test

ultra-high durability bridge is the Bessodani Bridge in the Tokushima Expressway [4]. This bridge was opened to traffic in December 2020. It is a 25.5 m long single-span bridge with the butterfly web box girder as shown in **Fig. 1**. This report presents the static and dynamic vehicle load testing using a 40-ton gross weight crane which was conducted to verify design consideration and evaluation of bridge structural performance. The validity of the design and the load-bearing performance of the structure were confirmed from the strain and displacement measured in the static load testing.

**Table 1.** Measuring parameters in static load testing

| No | Components | Parameters | Instruments |
|---|---|---|---|
| **1** | Slab concrete | Strain | KM strain transducer |
| **2** | Web concrete | Strain | Foil strain gauge |
| **3** | Web AFRP | Strain | Metal backing strain gauge |
| **4** | Deviator GFRP | Strain | Metal backing strain gauge |
| **5** | Segmental joint | Displacement | Crack disp. transducer |

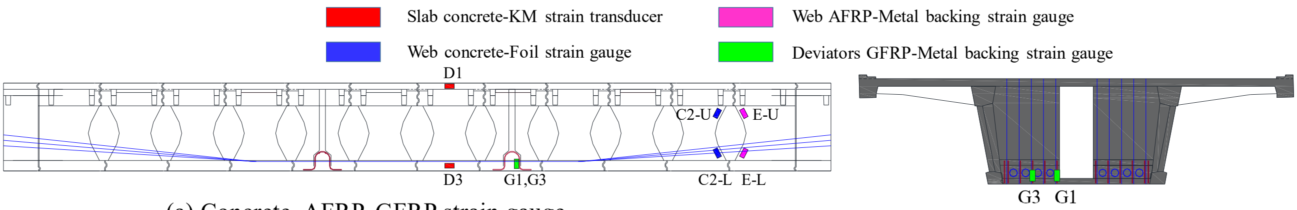


(a) Concrete, AFRP, GFRP strain gauge

(b) GFRP strain gauge

**Fig. 3.** Measuring instrument in static load testing

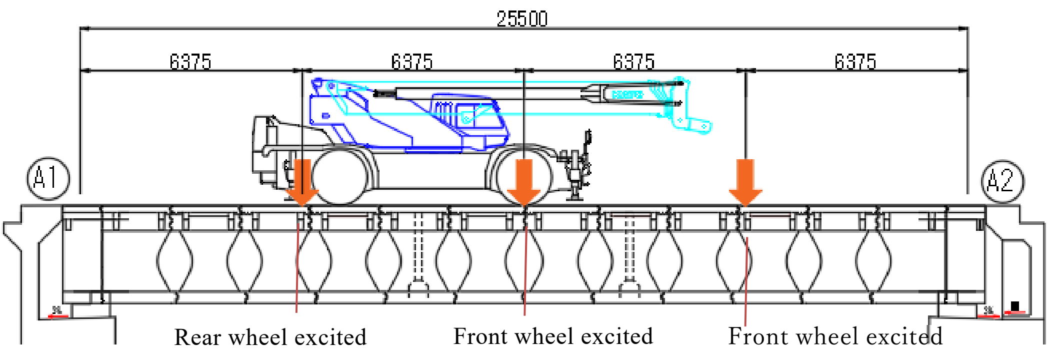


(a) Impact load position

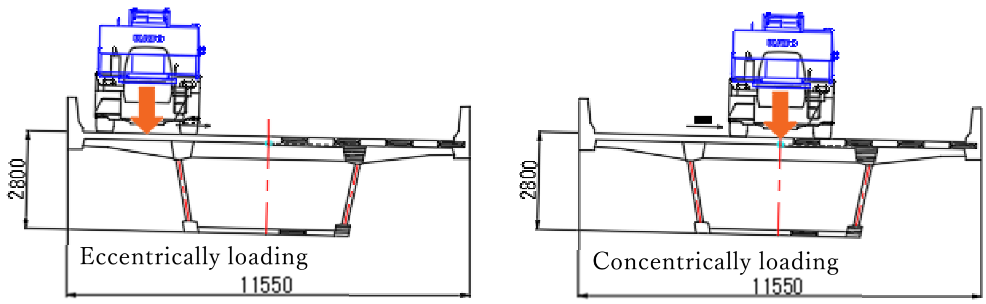


(b) Load position on deck slab

**Fig. 4.** Loadings for dynamic test

Furthermore, vibration load testing was also conducted by dropping the vehicle on the slab to identify the dynamic characteristics of the bridge as well as estimate the tension in AFRP external cables. The automated real-time monitoring system which is operating to monitor the long-term performance of the Bessodani Bridge was also explained in this paper.

## 2. LOAD TESTING

### 2.1 STATIC LOAD TESTING

The static load testing was conducted by a rough terrain crane with a total weight of 40 tons. To confirm the design in the longitudinal direction, the center of gravity of the vehicle was loaded at one-fourth, half, and three-fourth of the span

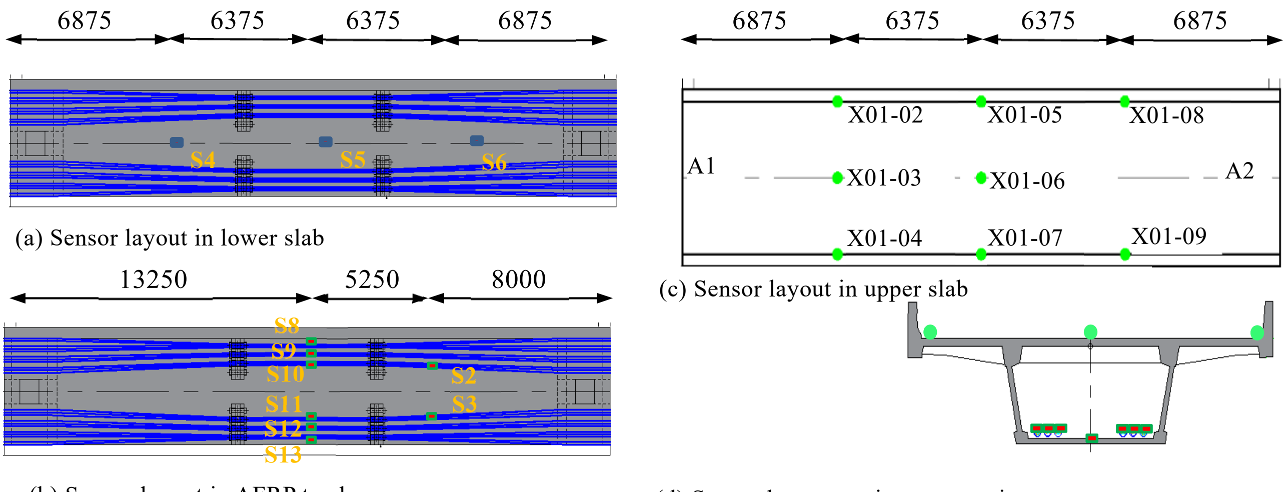


(a) Sensor layout in lower slab

(b) Sensor layout in AFRP tendons

(c) Sensor layout in upper slab

(d) Sensor layout out in cross section

**Fig. 5.** Measuring instrument in dynamic load testing

**Table 2.** Static load test strain result

($\times 10^{-6}$)

| No | Loading | Upper slab | Lower slab | Butterfly web | | Web AFRP rod | | GFRP rod | |
|---|---|---|---|---|---|---|---|---|---|
| | | D1 | D3 | C2-U(/) | C2-L(\) | E-U(\) | E-L(/) | G1 | G3 |
| **Case1** | L/4, center | -6 | +10 | +8 | -17 | -6 | +19 | +191 | +750 |
| **Case2** | **L/2, center** | **-9** | **+17** | **+19** | **-28** | **-16** | **+28** | **+188** | **+709** |
| **Case3** | 3L/4, center | -7 | +11 | +14 | -30 | -19 | +33 | +190 | +719 |
| **Case4** | L/4, cantilever | -3 | +8 | +0 | -6 | +5 | +6 | +196 | +763 |
| **Case5** | L/2, cantilever | -5 | +14 | +6 | -14 | +1 | +14 | +204 | +748 |
| **Case6** | 3L/4, cantilever | -3 | +10 | +7 | -14 | -4 | +17 | +204 | +750 |
| **Case7** | L/4, joint | -5 | +9 | +9 | -12 | -7 | +10 | +192 | +750 |
| **Case8** | L/2, joint | -3 | +16 | +26 | -31 | -18 | +28 | +187 | +724 |
| **Case9** | 3L/4, joint | -5 | +9 | +14 | -20 | -12 | +19 | +190 | +733 |
| **Case 0 (Design)** | L/2, center | -7.9 | +22.9 | +31.8 | -31.8 | -31.8 | +31.8 | ≦+2098 | ≦+2098 |

*Note:* + sign means tensile, - sign means compression.

of the bridge as shown in **Fig. 2(a)**. The loading was introduced both concentrically and eccentrically by loading the crane at deck central and deck cantilever as in **Fig. 2(c)** in the test of longitudinal direction, making 6 loading test cases from Case 1 to Case 6. In addition, the rear wheel in Case 7, 8 or front-wheel in Case 9 was set right above the segment joint to confirm the segment joint, as shown in **Fig. 2(b)**. The loading was introduced in central of upper deck to form 3 studied cases, Case 7 to Case 9, for the joint test. Hence, there are the total of 9 loading cases in the static load testing. Deck slab concrete strain, web AFRP rod strain, and web concrete strain were measured by instruments as shown in **Table 1**. The strain in glass fiber reinforced polymer GFRP which reinforced external cable deviator was also recorded. The segment joint is checked by measuring the relative displacement between segments. The measuring instrument layout is shown in **Fig. 3**.

## 2.2 DYNAMIC LOAD TESTING

The purpose of the dynamic load test is to identify the dynamic vibration characteristics of the bridge and external AFPR tendons. The main dynamic parameters of the bridge are natural frequencies, modal shapes. The main dynamic characteristics of external AFRP cables are natural frequencies that allow estimating residual tension prestress in the cables. The dynamic load testing is performed by

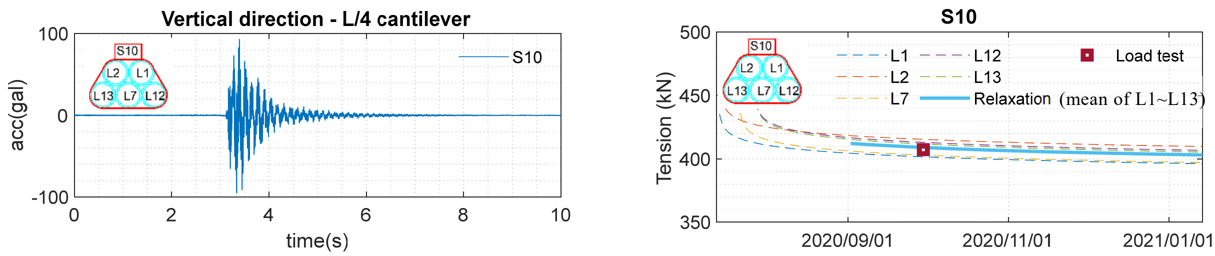


(a) Acceleration in FRP cables (b) Estimated tension force s of FRP cables

**Fig. 6.** Estimation of tension stress of FRP external cables

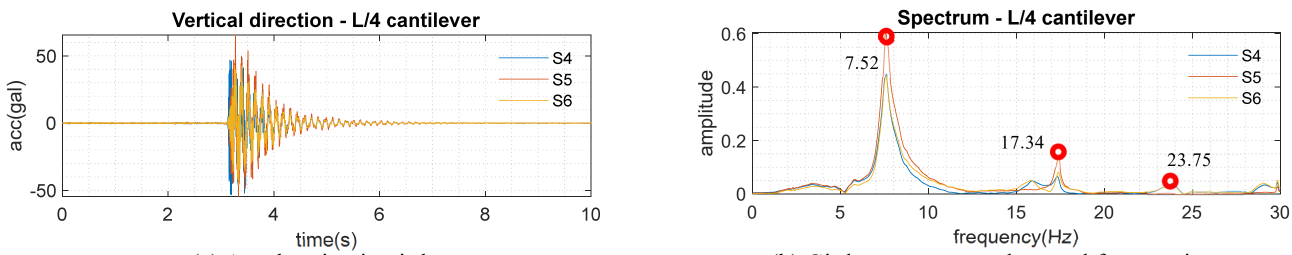


(a) Acceleration in girder (b) Girder spectrum and natural frequencies

**Fig. 7.** Bridge natural frequency identification

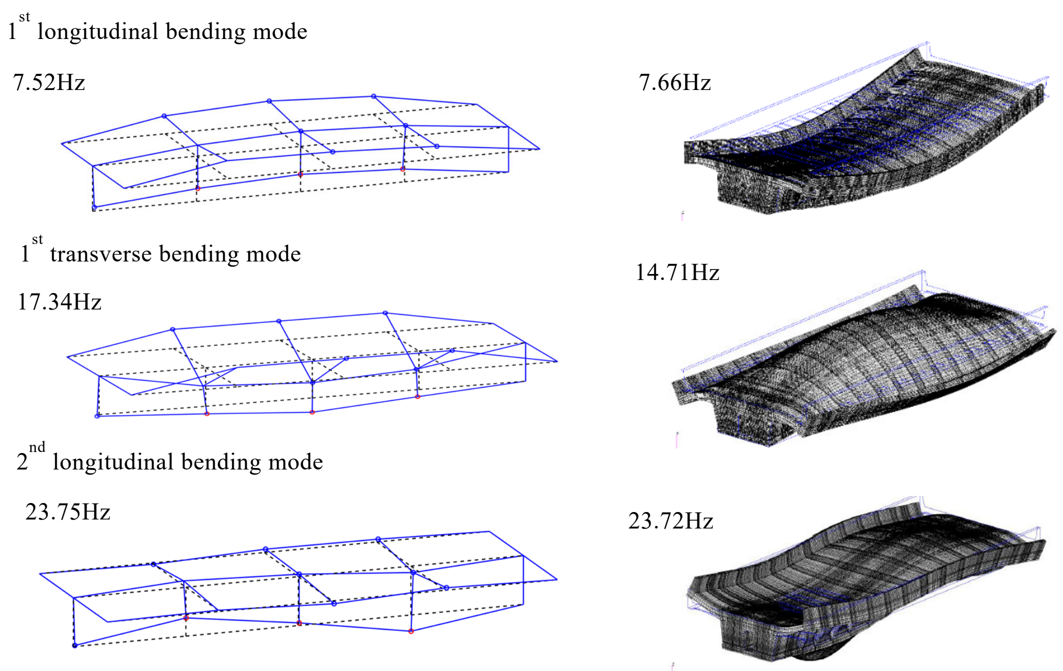


(a) Measurement results (b) Calculation results

**Fig. 8.** Vibration modal shapes

dropping the crane on upper slab to make the impacted vibration of the bridge. The same crane with the static load testing, which has a 40-ton gross weight, was employed. Total eighteen excited cases were conducted in three-time repetition with the excitation location at one-fourth, half, and three-fourth of girder span. The front wheels were stepped on slope which is approximately 20 cm in height installed at half, and three-fourth of the girder span. Then the crane was dropped down from top of the slope to slab to excite the vibration of the bridge. The same process was conducted to excite the bridge at one-fourth of the girder span with rear wheel stepping on the slope. Both concentric and eccentric excitation on the deck slab was performed as **Fig. 4**. The acceleration of abutment, girder, deck and external cables was measured by a set of accelerometers as shown in **Fig. 5** with a sampling of 800Hz.

## 3. LOAD TESTING RESULTS

### 3.1 STATIC LOAD TESTING RESULTS

**Table 2** shows representative measurements of the deck slab concrete strain, butterfly web concrete strain, web AFRP rod strain, and GFRP rod strain in static load testing. Under crane static loading at half-span, deck center position, the strain in upper deck slab concrete D1 is -9μ, and lower deck slab D3 is 17μ as shown in Case 2. It is consistent with the value in design value of -7.9μ and 22.9μ respectively as shown in Case 0, designed calculation using simple beam model with section area of 3.997 $m^2$, second moment of area of 4.31 $m^4$ and the actual measurement value of Young's modulus of 41400 $N/mm^2$. The strain results in butterfly web concrete, as well as strain of web ARFP rod, are also agreed with design value. The strain in GFRP which reinforced external cable deviator concrete is confirmed much lower than the limit value. The relative displacements between segments also confirmed the joint is not opened when the crane load just above the joint. Hence, the bridge's load-carried performance is validated, and the design calculation is confirmed reasonable.

### 3.2 DYNAMIC LOAD TESTING RESULTS

The effective prestress in AFRP tendons is needed to be measured but hardly measured by the strain gauge. In this bridge, the external tendon's tension is measured by a vibration-based method which is presented in detail in reference 5). **Fig. 6(a)** shows representative acceleration and estimated prestress in tendons at sensor S10 when crane impacted at L/4 span, cantilever deck slab. The S10 sensor measures the vibration of five-tendons L1, L2, L7, L12, L13 which has 9ϕ7.4 AFRP rods in each tendon. The tension is estimated for the current effective prestress in a 9ϕ7.4 AFRP rods which represents averaged value of five-tendons L1, L2, L7, L12, L13 as shown in **Fig. 6(b)**. This tension is the result calculated by equation (1) with uniform weight m in 1.2237kg/m, cable free vibration length L in 5.750m and the first natural frequency in 48.773Hz. Relaxation factor $\alpha(t)$ of tension in AFRP tendons is calculated by equation (2) where $t$ is relaxation period of the cable in hours. It confirms that the estimated prestress is well agreed with the calculation which accounted for relaxation of the AFPR rods. Similarly, **Fig. 7** shows an example of acceleration and the spectrum of the girder. Such dynamic properties of the bridge as natural frequencies and modal shapes, including first longitudinal bending mode, first transverse bending modes, and second longitudinal mode are identified as shown in **Fig. 8**. The identified natural frequencies and modal shapes are consistent with FEM analysis. The effective cable stressing, as well as dynamic properties, achieved from dynamic testing is foundation data for this bridge health monitoring.

$$\mathrm{T} = 4m\mathrm{L}^2\left(\frac{f_n}{n}\right)^2 \tag{1}$$

$$\alpha(t) = 0.95 - 0.031\log(t) \tag{2}$$

## 4. BRIDGE CONDITION MONITORING

### 4.1 MONITORING SYSTEM

To monitor the long-term performance of the Bessodani Bridge, a real-time automated monitoring system was installed and operated in the bridge. The system includes three sub-systems as shown in **Fig. 9**. The first sub-system is gauge and transducer system to monitor the strain of concrete components such as deck slab and web concrete, the strain of AFRP rods in web, and GFRP strain cable deviators. The segment joint is checked by measuring the relative displacement between segments in the first sub-system. The second sub-system is accelerometer system including several accelerometers are installed in girder, external cable, and abutment to monitor girder dynamic characteristics, cable tension, and detecting seismic and impact events in real-time. The third sub-system includes cameras which provide a remote observation ability for inspectors at any time. All the data is collecting in the cloud by mobile circuit. Data is visualized on the cloud which can be accessed from mobiles, tablets or desktops. If any seismic event, impacted event on the bridge, or any anomalies in cable tension or relative displacement between segment joints would be detected, the alert notification will be mailed to the bridge administration and inspectors in real-time.

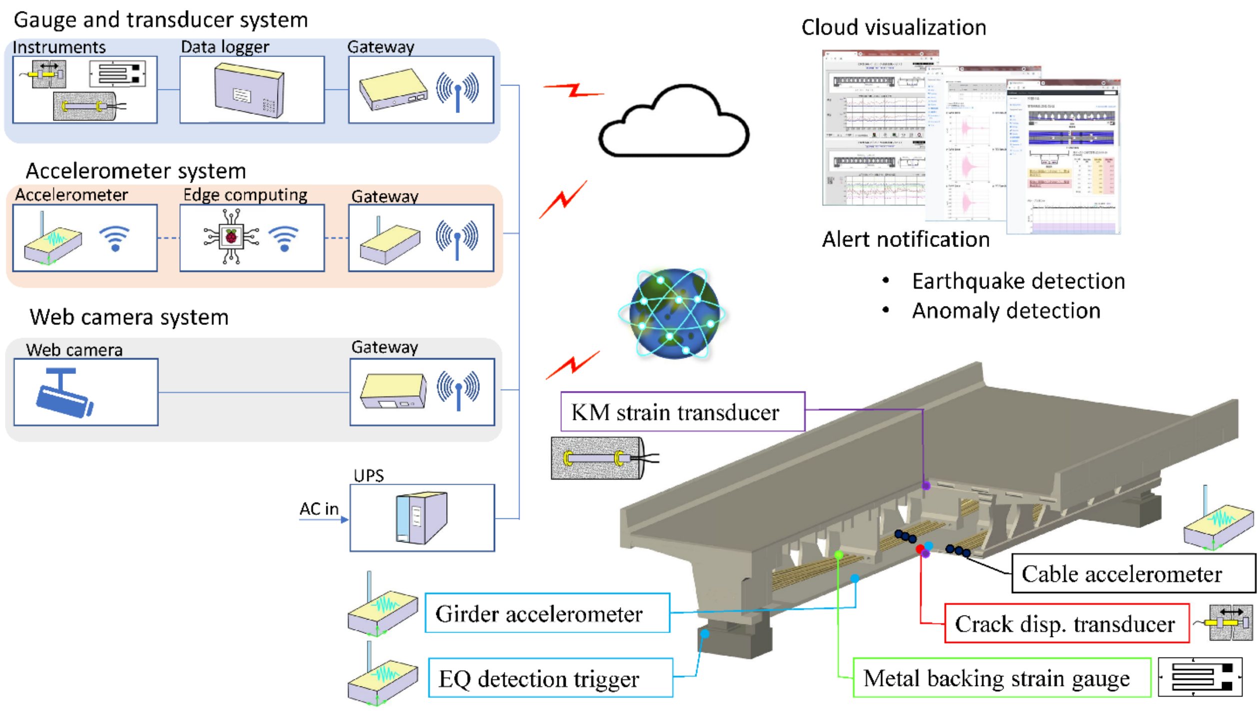


**Fig. 9.** Automated real-time monitoring system in the Bessodani Bridge

**Table 3.** Indicators for bridge condition monitoring

| No | Indicators | Instruments | Threshold |
|---|---|---|---|
| 1 | Earthquake detection | Accelerometers | Earthquake intensity |
| 2 | AFRP cable tension | Accelerometers | Cable tension |
| 3 | Segmental joint | Crack displacement transducer | Crack width |

### 4.2 EXTREME EVENT DETECTION

Detecting earthquake and intensity estimation was designed as a key function of the monitoring presented in this paper. The trigger nodes setting at abutment track the occurrence of the earthquake. Earthquakes are detecting by tracking RMS acceleration in the trigger node. If RMS acceleration becomes larger than a predefined threshold, an earthquake will be defined to occur, and the alert email will be sent the bridge administration and inspectors.

### 4.3 CONDITION MONITORING

Anomaly detection and bridge condition monitoring are critical key functions of the monitoring system in the Bessodani Bridge. The strain and displacement are collecting every hour and acceleration is measuring continuously. Based on these data, the condition of the bridge is automatedly monitoring in real-time through three indicators as shown in **Table 3**. Detail of anomaly detection algorithm can be found in reference 6). If measured values of any indicators excess their threshold, the system will mail an alert to bridge admission and inspectors in real-time.

## 5. CONCLUSION

This report presents the static and dynamic load testing of the Bessodani Bridge, the first ultra-high durability highway bridge, using a 40-ton gross weight crane. The consistency of strain and displacement measured in static test with calculated values confirms the design and the bridge performance. Prestress in AFRP external tendons, which are estimated by dynamic load testing, confirms an agreement with stress relaxation loss in design. The dynamic properties of the bridge such as natural frequencies and modal shapes are also identified. An automated real-time monitoring system integrated with strain gauges, displacement transducers, accelerometers, and web cameras were operated to monitor the performance of the bridge in real-time. Based on foundation data achieved from bridge testing, the condition of the bridge is monitored through several indicators in real-time. The system also integrated cloud technology to give a data access and visualize data at any time from mobiles, tablets or desktops. Alert notation will be mailed to bridge administration and inspectors when any abnormal condition of the bridge is detected in real-time.

**Acknowledgement:** The Bessodani Bridge is the achievement of joint research between Sumitomo Mitsui Construction Co., Ltd and West Nippon Expressway Co., Ltd. To confirm the long-term performance of the bridge, the monitoring system presented in this paper was installed and put in operation. Sensing network in this system is as a part of the joint research between Sumitomo Mitsui Construction Co., Ltd and Sonas Inc., Authors express their sincere gratitude to cooperation from these co-researchers.

**References**

1) Ogata, T., et al. “Development and construction of Ultra-durable bridges.”, Concrete Engineering, Vol. 54, No.4, pp.387-392, 2016.

2) Kasuga, A. : “Effects of butterfly web design on bridge construction”, Structural Concrete, Vol.18, pp. 128–142, 2017.

3) Asai, H. : “Research on practical application of adhesively anchored aramid fiber as tensioning and reinforcing material”, Doctoral thesis, Tokushima University, 2012.

4) Matsuo, Y., Wada, Y., Fujioka, T., Nagamoto, N.: “Construction of non-metal bridge”, the fib Symposium 2021, 2021.

5) Uchibori, H., Khuyen, H. T., and Nagamoto, N.: “Vibration based method for estimating stress in AFRP external cables”, the 29th Symposium on the Development of Prestressed Concrete, 2020.

6) Khuyen, H. T., et al. “Vibration-based anomaly detection method for structural health monitoring of in-service structures under ambient vibration”, Bridge Maintenance, Safety, Management, Life-Cycle Sustainability and Innovations, CRC Press, pp.3547-3554, 2021.